

Uranium symmetric/asymmetric neutron-induced fission up to 200 MeV

V.M. Maslov^a

Joint Institute for Nuclear and Energy Research, “Sosny”, 220109, Minsk, Belarus

Received: 26 August 2003 / Revised version: 31 January 2004 /

Published online: 17 August 2004 – © Società Italiana di Fisica / Springer-Verlag 2004

Communicated by A. Molinari

Abstract. The symmetric SL-mode and asymmetric lumped (S1 + S2)-mode fission cross-sections of $^{235}\text{U}(\text{n}, \text{F})$ and $^{233}\text{U}(\text{n}, \text{F})$ reactions are calculated up to $E_n = 200$ MeV within a statistical model. For each U nuclide, emerging in (n, xnf) reactions a separate triaxial outer fission barrier is assumed for the SL-mode. To reproduce the measured branching ratio of symmetric and asymmetric fission events for the $^{238}\text{U}(\text{n}, \text{F})$ reaction, more fissions coming from neutron-deficient nuclei were assumed. The damping of the triaxial collective modes contribution to the level density at the SL-mode outer saddle was essential for the branching ratio description. These assumptions allow to reproduce observed fission cross-sections of $^{235}\text{U}(\text{n}, \text{F})$ and $^{233}\text{U}(\text{n}, \text{F})$ reactions. The calculated branching ratio sensitivity to the target nuclide fissility is investigated.

PACS. 24.10.Pa Thermal and statistical models – 25.85.Ec Neutron-induced fission – 24.75.+i General properties of fission

1 Introduction

In the neutron-induced fission reaction of actinides when the incident neutron energy is higher than the emissive fission threshold, pre-saddle (n, xnf) neutrons might be emitted. This happens before the fissioning nuclide reaches the outer saddle point of the double-humped fission barrier [1]. This peculiarity much complicates the interpretation of the fission observables, since they correspond to an ensemble of fissioning actinide nuclides. Pre-scission neutrons might be emitted also during saddle-to-scission transition. However, the contribution of these neutrons is relatively lower than that of the pre-saddle neutrons. For the $^{238}\text{U}(\text{n}, \text{xnf})$ fission reaction at $E_n \sim 200$ MeV the number of nuclides contributing to the fission observables might be ~ 20 [2]. That means the mass and excitation energy of the actual fissioning nuclide are not known exactly. On the other hand, the fission fragments, formed after scission, could emerge in, at least, “two-mode” fission process, *i.e.*, symmetric and asymmetric mass division may take place [3, 4]. Superlong (SL) mode fission cross-sections [5, 6] of $^{235}\text{U}(\text{n}, \text{f})^{\text{sym}}$ and $^{238}\text{U}(\text{n}, \text{f})^{\text{sym}}$ fission reactions, related to the symmetric scission, were reproduced recently within a Hauser-Feshbach statistical model [7] for incident neutron energies below the emissive fission thresholds. The double-humped fission barrier model [1] was employed previously for the analysis

of the fission probability of Ac and Ra nuclei [8, 9]. It was concluded that symmetric fission “involves a separate outer barrier, which is assumed to be axially asymmetric”. In case of U nuclei, different threshold energies of the symmetric and asymmetric fission also could be correlated with the heights of the outer saddle points of the double-humped fission barrier. The shape of the fissioning nuclide at the saddle point strongly influences the energy dependence of either symmetric and asymmetric calculated fission cross-sections. A separate outer barrier *B* was assumed for the SL-mode, while a common inner barrier *A* was assumed for the symmetric SL- and lumped asymmetric (S1+S2)-mode. This assumption is supported by the fission mode calculations [10, 11] using the multimodal random-neck rupture model [3]. The SL-mode fission cross-section is controlled by rather high outer fission barrier E_{fBSL} with significant transparency, defined by the curvature parameter $\hbar\omega_{\text{fBSL}}$. The outer saddle point *B* triaxiality and mass symmetry lead to a steeper increase of the symmetric fission cross-section. The outer saddles for asymmetric S1- and S2-modes were assumed axially symmetric and mass asymmetric. Competition of the symmetric and asymmetric fission of the ^{234}U nuclide was investigated recently by Moller *et al.* [4] by modelling the multi-dimensional potential energy surface in a shell correction model.

We will assume that the ensemble of U nuclides, which might emerge after emission of *x* pre-saddle neutrons,

^a e-mail: maslov@sosny.bas-net.by, maslov@bas-net.by

contributes to the symmetric and asymmetric fission reactions. We will denote the neutron-induced fission reaction as (n, F) , to distinguish it from the non-emissive (first-chance) fission reaction (n, f) . The branching ratio of the symmetric fission events to the observed fission events $r^{\text{sym}} = \sigma_{\text{nFSL}} / (\sigma_{\text{nFSL}} + \sigma_{\text{nF(S1+S2)}})$ was obtained for $^{238}\text{U}(n, F)$ reaction by Zoller *et al.* [12] for E_n up to ~ 500 MeV. The branching ratio for the $^{238}\text{U}(n, F)$ reaction was obtained from the deduced yield distributions of the primary fission fragments and their average total kinetic energies $\langle TKE \rangle$, measured as a function of mass. The observed $^{238}\text{U}(n, F)$ fission cross-section data [13, 14] were reproduced recently [15] in a fission/neutron evaporation approximation up to $E_n \sim 200$ MeV. The present statistical model calculations of fission reaction cross-section assume fission/neutron evaporation competition during the decay of the excited compound nucleus, which is formed after first-chance emission of the pre-equilibrium (PE) neutron [16], treated with a simple version of the exciton model [17, 18]. The equilibration process is treated with a set of master equations, describing the evolution of the excited nucleus states, classified by the number of particles plus holes [16]. Damping of the collective modes contribution to the level density at excitations $U \gtrsim 20$ MeV for axial symmetric saddle and equilibrium deformations [19] is essential for the $^{238}\text{U}(n, F)$ data fit. Recently the branching ratio r^{sym} for the $^{238}\text{U}(n, F)$ reaction was reproduced up to $E_n \sim 200$ MeV [2]. It was shown that the branching ratio r^{sym} is much dependent also on the damping of the triaxial deformations influence on the level densities for the outer SL-mode saddles [2]. However, the branching ratio r^{sym} turned out to be even more dependent on the emissive fission chances contributions to the observed cross-section. Description of the r^{sym} ratio data by Zoller *et al.* [12] favours the predominant contribution to the observed fission cross-section of emissive fission chances with higher number x of pre-saddle neutrons. With increase of the target nuclide fissility the number x of pre-fission neutrons might somewhat decrease.

We will apply the statistical theory approach, tested by the description of the $^{238}\text{U}(n, F)$ observed fission cross-section and the branching ratio of symmetric/asymmetric fission, for the $^{235}\text{U}(n, F)$ and $^{233}\text{U}(n, F)$ observed fission cross-section data description. We will predict also $^{235}\text{U}(n, F)^{\text{sym}}$, $^{233}\text{U}(n, F)^{\text{sym}}$ and $^{235}\text{U}(n, F)^{\text{asym}}$, $^{233}\text{U}(n, F)^{\text{asym}}$ fission cross-sections. The advantage of this procedure is that no additional parameters are used, except those already fixed by the description of the $^{238}\text{U}(n, F)$ observed fission cross-section and branching ratio of symmetric/asymmetric fission.

2 Statistical model

The detailed description of the statistical model for the symmetric/asymmetric fission cross-section calculation in the emissive fission domain is given elsewhere [2]. Below a brief outline of the model is given. We assume that the emissive fissions come from a chain of U nuclei. This means that only PE-emission/evaporation of

neutrons is allowed [16]. For incident neutron energies up to $E_n \sim 20$ MeV the partitioning of the observed fission cross-section into emissive fission chances could be accomplished quite unambiguously in case of the $^{238}\text{U}(n, F)$ reaction. It was shown in [20], that consistent description of (n, F) , $(n, 2n)$, $(n, 3n)$ reaction cross-sections and prompt fission neutron spectra could be achieved within a convenient statistical model. A coupled channel model, fitting ^{238}U total data [21] up to $E_n \sim 200$ MeV is employed for the neutron transmission coefficients calculation. The SL-mode contribution to the observed fission cross-section, coming from the (n, xnf) fission reactions could be calculated using the fission probability $P_{\text{fSL}x}^{J\pi}(U)$ of the symmetric scission of fissioning x -th nucleus,

$$\sigma_{\text{nFSL}}(E_n) = \sigma_{\text{nfSL}}(E_n) + \sum_{x=1}^X \sum_{J\pi} \int_0^{U_{x+1}^{\text{max}}} W_{x+1}^{J\pi}(U) \times P_{\text{fSL}(x+1)}^{J\pi}(U) dU, \quad (1)$$

$W_x^{J\pi}(U)$ is the population of the $(x+1)$ -th nucleus, emerged after emission of x neutrons, at the excitation energy U . The excitation energy U_{x+1}^{max} depends on the incident neutron energy E_n and the energy, removed by the pre-saddle evaporated neutrons, *i.e.*, binding and kinetic energies. We do not take into account the charged-particle emission, for justification see discussion in [2]. The behavior of the first-chance fission cross-section σ_{nfSL} is obviously related to the energy dependence of the first-chance fission probability P_{nfSL} of the composite $A+1$ nuclide:

$$\sigma_{\text{nfSL}} = \sigma_r(1 - q(E_n))P_{\text{nfSL}}, \quad (2)$$

$q(E_n)$ being the contribution of the first neutron pre-equilibrium emission. The first-chance fission probability P_{nfSL} depends only on the level densities $\rho(U, J, \pi)$ of the fissioning $A+1$ and the residual A uranium nuclides. For more details about the first-chance fission cross-section σ_{nfSL} modelling see [7] and references therein. Lumped contribution to the observed fission cross-section of the asymmetric fission (S1+S2)-modes could be defined in an analogous way.

The nuclear level density $\rho(U, J, \pi)$ is represented as the factorized contribution of the quasiparticle and collective states [22] as

$$\rho(U, J, \pi) = K_{\text{rot}}(U)K_{\text{vib}}(U)\rho_{\text{qp}}(U, J, \pi), \quad (3)$$

quasiparticle level densities $\rho_{\text{qp}}(U, J, \pi)$ were calculated with a phenomenological model by Ignatyuk *et al.* [23], where $K_{\text{rot}}(U, J)$ and $K_{\text{vib}}(U)$ are factors of the rotational and vibrational enhancement. At saddle and ground-state deformations factor $K_{\text{rot}}(U)$ is defined by the deformation order of symmetry, adopted from the shell correction model calculations [24]. At excitations $U \geq U_r$, damping of the rotational modes was anticipated [25]. The damping might be different for the axially symmetric and triaxial nuclei [19], *i.e.*

$$K_{\text{rot}}^{\text{sym}}(U) = (\sigma_{\perp}^2 - 1)F(U) + 1, \quad (4)$$

$$K_{\text{rot}}^{\text{asym}}(U) = K_{\text{rot}}^{\text{ax}}(U)((2\sqrt{2}\pi\sigma_{\parallel} - 1)F(U) + 1), \quad (5)$$

$$F(U) = (1 + \exp(U - U_r)/d_r)^{-1}. \quad (6)$$

Here, σ_{\parallel}^2 and σ_{\perp}^2 are spin distribution parameters. The mass asymmetry for the S1(S2)-modes at outer saddles doubles the rotational enhancement factors as defined by eqs. (4), (5). The shell effects in level density are modelled with the shell correction δW dependence of the a -parameter as recommended by Ignatyuk *et al.* [23]: $a = a(U) = \tilde{a}(1 + \delta W f(\tilde{U})/\tilde{U})$. The value of the main a -parameter is defined by fitting the neutron resonance spacing $\langle D_{\text{obs}} \rangle$ or systematics [26] for the U nuclei: $\tilde{a}/A = -0.1798 + 0.0012A$. We assume that $\tilde{a}_n = \tilde{a}_f$, then a_f/a_n ratio would depend on the shell correction values $\delta W_{f(n)}$. The respective values are taken from [27] (δW_n) and [28] (δW_f). We assume a rather strong damping of the axial symmetric rotational mode contribution $K_{\text{rot}}^{\text{sym}}(U)$ both at equilibrium and saddle deformation, *i.e.* the parameters used in eq. (6) are $U_r = 20$ MeV and $d_r = 5$ MeV. For triaxial damping modelling, *i.e.*, to calculate $K_{\text{rot}}^{\text{asym}}(U)$, the parameters of eq. (6) are $U_r = 30$ MeV and $d_r = 10$ MeV. For more details see previous papers [2, 7].

3 Analysis

The observed fission cross-section $\sigma_{\text{nF}} = \sigma_{\text{nFSL}} + \sigma_{\text{nF(S1+S2)}}$ depends on the contributions of the emissive fission to both symmetric σ_{nFSL} and asymmetric $\sigma_{\text{nF(S1+S2)}}$ fission terms. These contributions are strongly dependent on the asymptotic value $\tilde{a}_f(A)$ of the a_f parameter of U nuclei, which is used for the calculation of the fission probabilities $P_{f(x+1)}^{J\pi}(U)$. The branching ratio r^{sym} depends on both the contributions of the emissive fission chances. Damping of the triaxial collective modes for the SL-mode fission was introduced to fit the measured data trend for the $^{238}\text{U}(\text{n}, \text{F})$ reaction. Contributions of the emissive fission chances to the observed fission cross-section σ_{nF} are affected by the asymptotic value of the a_f parameter, decreasing with energy as

$$\tilde{a}_f(U, A) = \tilde{a}_f(A) \left(1 - 0.1 \left(\frac{U - 20}{U} \right)^{1/4} \right). \quad (7)$$

This decrease of $\tilde{a}_f(U, A)$ leads to a major redistribution of the contributions of chance fission reactions to the observed fission cross-sections. The SL-mode outer fission barrier B parameters for the ^{239}U and ^{236}U fissioning nuclei were derived to be higher than those of asymmetric modes, *i.e.* $(E_{\text{fBSL}} - E_{\text{fBS1(S2)}}) \sim 3.5$ MeV, while $\hbar\omega_{\text{BSL}} = 2.25$ MeV [7]. The contributions of the lower mass U nuclides via the (n, xnf) reaction to the observed symmetric fission might be obtained assuming for each of them the same difference of the outer barriers for symmetric SL and asymmetric fission S1(S2)-modes. The shell correction values are defined as $(\delta W_{\text{fBSL}} - \delta W_{\text{fBS1(S2)}}) \sim 3.5$ MeV, for the asymmetric mode fission $\delta W_{\text{fBS1(S2)}} \sim 0.6$ MeV is assumed [28]. The assumption that the difference of the mass-symmetric and mass-asymmetric fission barriers for uranium nuclei does not vary with the neutron number might seem excessively crude (see Schmidt *et al.* [29]),

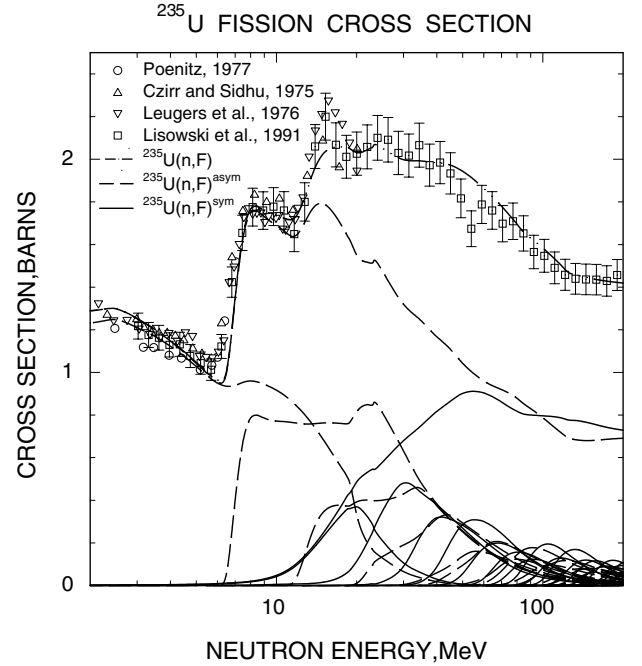


Fig. 1. $^{235}\text{U}(\text{n}, \text{F})$ cross-section. The dashed lines show asymmetric fission cross-sections; the solid lines show symmetric fission cross-sections; the dot-dashed line shows the sum of symmetric and asymmetric fission cross-sections. The asymptotic value $\tilde{a}_f(U, A)$ of the a_f parameter is employed (eq. (6)), triaxial damping at the outer SL-mode saddle is assumed (eqs. (3)-(5)).

however, we believe that the anticipated weak isotopic dependence of $(E_{\text{fBSL}} - E_{\text{fBS1(S2)}})$ could be compensated by slight variation of the asymptotic value of the a_f parameter (see eq. (7)). Uranium inner and outer fission barrier parameters relevant for the asymmetric fission, for the saddle asymmetries predicted by SCM calculations [24], were defined in [30, 31]. This simple systematics of level density and fission barrier parameters for the U nuclides allowed to reproduce the observed $^{238}\text{U}(\text{n}, \text{F})$ fission cross-section and the symmetric/asymmetric branching ratio r^{sym} . The same approach would be applied to describe neutron-induced fission cross-sections of ^{233}U and ^{235}U target nuclides for incident neutron energies up to 200 MeV.

3.1 $^{235}\text{U}(\text{n}, \text{f})$

Figure 1 shows the calculated symmetric $^{235}\text{U}(\text{n}, \text{F})^{\text{sym}}$, asymmetric $^{235}\text{U}(\text{n}, \text{F})^{\text{asym}}$ and symmetric + asymmetric $^{235}\text{U}(\text{n}, \text{F})$ fission cross-sections. The damping of axial deformations with $U_r = 20$ MeV and $d_r = 5$ MeV and the damping of triaxial deformations with $U_r = 30$ MeV and $d_r = 10$ MeV (eqs. (4)-(6)) at outer SL-mode saddles are assumed. The energy-dependent asymptotic value $\tilde{a}_f(U, A)$ of the a_f parameter (see eq. (7)) is employed. The measured data by Lisowski *et al.* [13] for the $^{235}\text{U}(\text{n}, \text{F})$ reaction are compatible with earlier measured data by Poenitz [32], Czirr and Sidhu [33] and Leugers *et al.* [34], which span the incident neutron energy range $E_n \lesssim 20$ MeV. The set of solid line curves shows

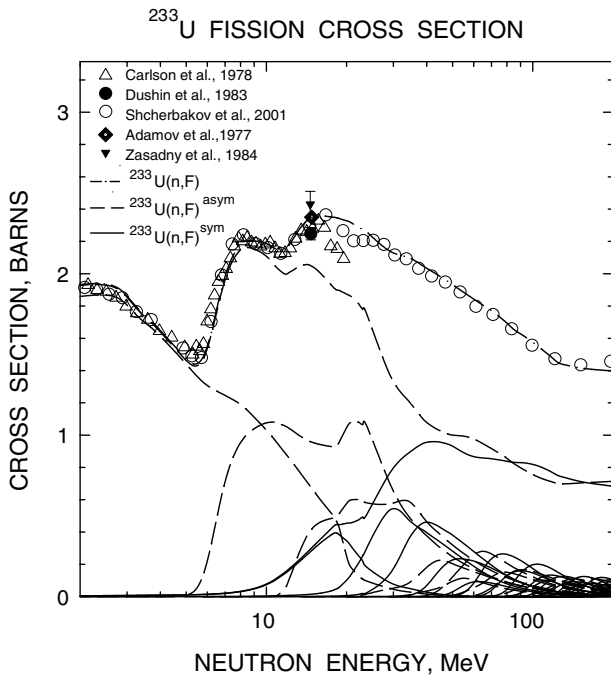


Fig. 2. $^{233}\text{U}(n, F)$ cross-section, same as in fig. 1.

$^{235}\text{U}(n, F)^{\text{sym}}$ and $^{235}\text{U}(n, xnf)^{\text{sym}}$ cross-sections, while the dashed lines show those for the asymmetric neutron-induced fission of the ^{235}U target nuclide. The sum of symmetric $^{235}\text{U}(n, F)^{\text{sym}}$ and asymmetric $^{235}\text{U}(n, F)^{\text{asym}}$ fission reaction cross-sections (dash-dotted line) is quite compatible with the observed fission cross-section data for the $^{235}\text{U}(n, F)$ reaction up to $E_n \sim 200$ MeV.

3.2 $^{233}\text{U}(n, f)$

The fissility of the ^{234}U nuclide is much higher than that of ^{236}U . Figure 2 shows symmetric $^{233}\text{U}(n, F)^{\text{sym}}$, asymmetric $^{233}\text{U}(n, F)^{\text{asym}}$ and symmetric + asymmetric $^{233}\text{U}(n, F)$ fission cross-sections. The lines in fig. 2 have the same meanings as those in fig. 1. There are quite a number of measured data for the $^{233}\text{U}(n, F)$ reaction cross-section, most of them span the incident neutron energy range $E_n \lesssim 20$ MeV, except recent data by Shcherbakov *et al.* [14], measured relative to the $^{235}\text{U}(n, f)$ reaction cross-section. However, original data by Shcherbakov *et al.* [14] are systematically (by 5–10%) higher than most of the available neutron-induced fission data for $E_n \lesssim 20$ MeV. For clarity, we showed in fig. 2 only measured data by Carlson and Behrens [35], measured relative to the $^{235}\text{U}(n, f)$ cross-section, and absolute data by Dushin *et al.* [36], Adamov *et al.* [37] and Zasadny *et al.* [38] at $E_n \sim 15$ MeV. Data by Shcherbakov *et al.* [14] are shown normalized to the absolute $^{233}\text{U}(n, F)$ fission data by Kalinin *et al.* [39] at $E_n = 1.9$ MeV. Sum of the calculated $^{233}\text{U}(n, F)^{\text{sym}}$ and $^{233}\text{U}(n, F)^{\text{asym}}$ reaction cross-sections (dash-dotted line) is quite compatible up to $E_n \sim 200$ MeV with the observed fission cross-section of $^{233}\text{U}(n, F)$ reaction up to $E_n \sim 20$ MeV and with re-normalized data by Shcherbakov *et*

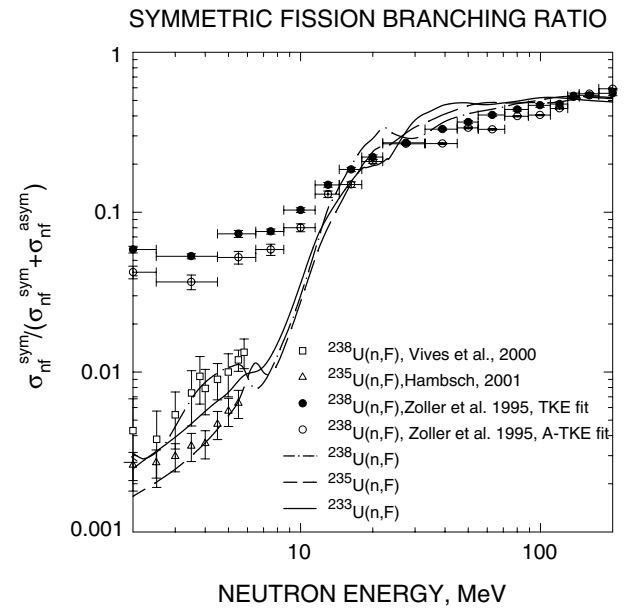


Fig. 3. Branching ratio r^{sym} of symmetric to symmetric plus asymmetric fission events of the $^{233}\text{U}(n, F)$ (solid line), $^{235}\text{U}(n, F)$ (dashed line) and $^{238}\text{U}(n, F)$ reaction (dot-dashed line). Symbols show measured data by Zoller *et al.* [12] and Vives *et al.* [6] for $^{238}\text{U}(n, f)$, Hamsch [5] for $^{235}\text{U}(n, f)$. Solid and dashed lines correspond to the energy-dependent asymptotic value $\tilde{a}_f(U, A)$ of the a_f parameter, defined using eq. (6); damping of triaxial deformations (eqs. (3)-(5)) is assumed.

al. [14]. Measured $^{233}\text{U}(n, F)$ fission data [14], normalized to absolute $^{233}\text{U}(n, F)$ fission data by Kalinin *et al.* [39] at $E_n = 1.9$ MeV are consistent also with the absolute data by Adamov *et al.* [37] at $E_n \sim 15$ MeV. Uranium nuclei, which give predominant contribution to the $^{233}\text{U}(n, F)$ reaction cross-section, are also important for the description of the $^{235}\text{U}(n, F)$ and $^{238}\text{U}(n, F)$ observed fission cross-sections. In other words, relevant fission barrier and level density parameters are already tuned to reproduce $^{235}\text{U}(n, F)$ and $^{238}\text{U}(n, F)$ data. It could be argued also that our estimate of the $^{233}\text{U}(n, F)$ observed fission cross-section is a theoretical prediction for incident neutron energies higher than $E_n \gtrsim 20$ MeV.

3.3 Branching ratio

The relative contributions of symmetric σ_{nF}^{sym} and asymmetric $\sigma_{nF}^{\text{asym}}$ modes to the observed fission cross-section σ_{nF} could be controlled by comparing the calculated branching ratio r^{sym} with measured data. In addition to the ratio data for the $^{238}\text{U}(n, F)$ reaction by Zoller *et al.* [12] (see fig. 3), there are measured data by Hamsch [5] for the $^{238}\text{U}(n, f)$ and Vives *et al.* [6] for the $^{235}\text{U}(n, f)$ reaction below the emissive fission thresholds. The relative contributions of fission chances with low and high number of the pre-fission neutrons strongly influence the energy dependence of the calculated r^{sym} at $E_n \gtrsim 25$ MeV. When the energy-dependent asymptotic $\tilde{a}_f(U, A)$ of a_f parameter is employed (see eq. (7)), higher fission chances give

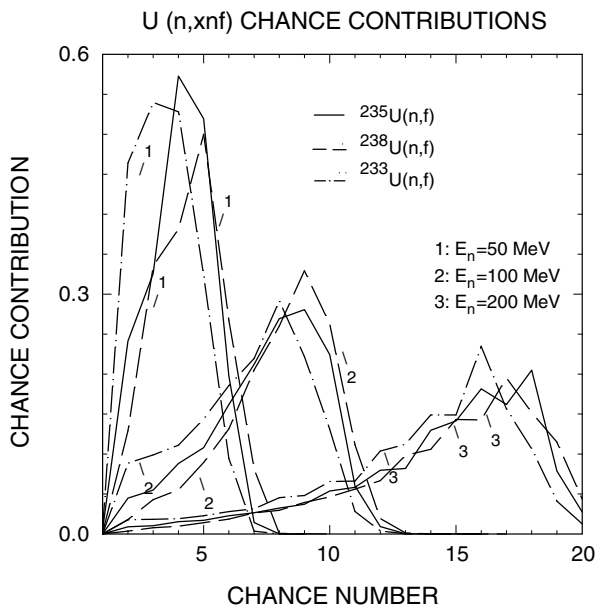


Fig. 4. Emissive chance fission distributions for $^{233}\text{U}(n,xf)^{\text{sym+asym}}$ (dot-dashed line), $^{235}\text{U}(n,xf)^{\text{sym+asym}}$ (solid lines) and $^{238}\text{U}(n,F)^{\text{sym+asym}}$ (dashed lines) reactions for the energy-dependent asymptotic value $\tilde{a}_f(U, A)$ of the a_f parameter (see eq. (6)). Triaxial damping at the outer SL-mode saddle is assumed (eqs. (3)-(5)).

predominant contribution to the observed fission cross-section. “Triaxial damping” of the collective modes contribution to the level density allowed to reproduce the measured data by Zoller *et al.* [12] for $^{238}\text{U}(n, F)$ at $E_n \gtrsim 10$ MeV; at lower energies the data are claimed to be too high by the authors [12] themselves. Below the emissive fission threshold there is a systematic difference of the branching ratio data by Hambsch [5] for $^{238}\text{U}(n, f)$ and Vives *et al.* [6] for $^{235}\text{U}(n, f)$. The branching ratio for the $^{233}\text{U}(n, f)$ reaction, calculated with fission barrier and level density parameter systematics is at the intermediate level.

The calculated branching ratios r^{sym} for $^{233}\text{U}(n, F)$, $^{235}\text{U}(n, F)$ and $^{238}\text{U}(n, F)$ reactions exhibit different shapes around relevant $^{233(235,238)}\text{U}(n, nf)$ reaction thresholds. A strong dip is predicted for the $^{238}\text{U}(n, F)$ reaction, a similar dip, but of lower amplitude, appears for the $^{235}\text{U}(n, F)$ reaction, while it almost disappears in case of the $^{233}\text{U}(n, F)$ reaction. These peculiarities are due to the different competition of the symmetric $\text{U}(n, F)^{\text{sym}}$ and asymmetric $\text{U}(n, F)^{\text{asym}}$ fission reactions, since the fission thresholds of the symmetric fission modes are higher as compared with those of the asymmetric fission. At incident neutron energies in the range of $25 \lesssim E_n \lesssim 60$ MeV symmetric fission gives the highest contribution to the observed fission cross-section in case of $^{233}\text{U}(n, F)$ reaction, but the lowest in case of $^{238}\text{U}(n, F)$ reaction. This effect might be explained by different emissive fission contributions to the $(n, F)^{\text{asym}}$ and $(n, F)^{\text{sym}}$ reactions in case of $^{233}\text{U}(n, F)$, $^{235}\text{U}(n, F)$ and $^{238}\text{U}(n, F)$ reactions. Emissive fission chances distributions for the different target nuclei are compared in fig. 4. It shows that the contribution of the

lower fission chances, *i.e.*, chances with lower number of pre-saddle neutrons at incident neutron energies $E_n = 50, 100$ and 200 MeV is the highest in case of ^{233}U target, but the lowest in case of ^{238}U target. In summary, the different shapes of branching ratios r^{sym} for $^{233}\text{U}(n, F)$, $^{235}\text{U}(n, F)$ and $^{238}\text{U}(n, F)$ reactions for $E_n \lesssim 60$ MeV might be attributed to the higher contributions of lower fission chances in case of higher target nuclide fissility; for higher energies they do not differ much.

4 Conclusions

The damping of the axial collective modes contribution to the level density both for inner and outer saddles and equilibrium deformations as well as the triaxial damping at the SL-mode outer saddle, produce symmetric/asymmetric emissive fission partitioning of $^{238}\text{U}(n, F)$, $^{235}\text{U}(n, F)$ and $^{233}\text{U}(n, F)$ reaction cross-sections. This is based on the consistent description of observed fission cross-sections and symmetric fission branching ratio for the $^{238}\text{U}(n, F)$ reaction. The present estimate of the energy-dependent level density parameter at saddle deformations is equivalent to more fission events at lower intrinsic excitation energies, or more fission events coming from the neutron-deficient U nuclei, *i.e.* from higher fission chances. The damping of triaxial collective modes contributions at the outer SL-mode saddle is equivalent to less symmetric fission events at higher excitation energy and more symmetric fission from neutron-deficient isotopes, as compared with the “no triaxial damping” case. The dependence of the symmetric fission branching ratio on the target nuclide fissility is interpreted as being due to the higher contribution of the lower fission chances in case of higher target nuclide fissilities. At the other extreme of the lower fissility target nuclei there are measured data for the $^{232}\text{Th}(n, F)$ reaction [14]. It turns out that the description of the observed fission cross-section also could be attained only in the case when more fissions come from neutron-deficient Th nuclei, *i.e.* from higher fission chances. In the opposite case the calculated $^{232}\text{Th}(n, F)$ fission cross-section would remain much higher than the measured data. The dependence of the symmetric fission branching ratio on the incident particle also could be explored within the present approach. The analysis of the proton-induced fission cross-section of the $^{238}\text{U}(p, F)$ reaction could be a viable candidate, relevant fission barrier and level density parameters of Np nuclei could be fixed to a large extent by the description of the $^{237}\text{Np}(n, F)$ data by Scherbakov *et al.* [14]. Summarizing, we might argue that a consistent description of the measured Th, U, Np and Pu neutron-induced fission cross-section data and measured symmetric fission branching ratio for the $^{238}\text{U}(n, F)$ reaction could be accomplished within the present statistical model.

It would be of much interest also to estimate the probability of symmetric fission in the $^{235}\text{U}(n, F)$ reaction [40] as a function of the internal excitation energy of the fissioning nuclei in the emissive fission domain. To accomplish that we should calculate exclusive $^{235}\text{U}(n, xnf)$ reaction

neutron spectra. These problems would be addressed as an extension of the present work.

This work was supported by International Science and Technology Center under the Project B-404 “Actinide Nuclear Data Evaluation”, Funding Party Japan, and International Atomic Energy Agency under Research Contract RC9837.

References

1. V.M. Strutinsky, Nucl. Phys. A **95**, 420 (1967).
2. V.M. Maslov, Nucl. Phys. A **717**, 3 (2003).
3. U. Brosa, S. Grossmann, A. Müller, Phys. Rev. **197**, 167 (1990).
4. P. Möller, D.G. Madland, A.J. Sierk *et al.*, Nature **409**, 785 (2001).
5. F.-J. Hamsch, private communication (2001).
6. F. Vives, F.-J. Hamsch, H. Bax, S. Oberstedt, Nucl. Phys. A **662**, 63 (2000).
7. V.M. Maslov, F.-J. Hamsch, Nucl. Phys. A **705**, 352 (2002).
8. E. Konecny, H.J. Specht, J. Weber, Phys. Lett. B **45**, 329 (1973).
9. J. Weber, H.C. Britt, A. Gavron *et al.*, Phys. Rev. **13**, 2413 (1976).
10. S. Oberstedt, F.-J. Hamsch, F. Vives, Nucl. Phys. A **644**, 289 (1998).
11. F.-J. Hamsch, F. Vives, P. Ziegler *et al.*, Nucl. Phys. A **679**, 3 (2000).
12. C.M. Zoller, A. Gavron, J.P. Lestone *et al.*, IKDA 95/25, Darmstadt.
13. P. Lisowski, A.D. Carlson, O.A. Wasson *et al.*, *Proceedings of the Specialists' Meeting on Neutron Cross Section Standards for the Energy Region above 20 MeV, Uppsala, Sweden, 21-23 May, 1991* (OECD, Paris, 1991) p. 177.
14. O.A. Shcherbakov, A. Donets, A. Evdokimov, A. Fomichev, T. Fukahori, A. Hasegawa, A. Laptev, V. Maslov, G. Petrov, S. Soloviev, Yu. Tuboltsev, A. Vorobyev, *Proceedings of the International Conference on Nuclear Data for Science and Technology, October 7-12, 2001, Tsukuba, Japan* (Atomic Energy Society, Tokyo, Japan, 2001) p. 230.
15. V.M. Maslov, Yu.V. Porodzinskij, A. Hasegawa, M. Baba, *Proceedings of the International Conference on Nuclear Data for Science and Technology, October 7-12, 2001, Tsukuba, Japan* (Atomic Energy Society, Tokyo, Japan, 2001) p. 80.
16. M. Uhl, B. Strohmaier, IRK-76/01, IRK, Vienna (1976).
17. C.K. Cline, Nucl. Phys. A **195**, 353 (1972).
18. E. Gadioli, E. Gadioli Erba, P.G. Sona, Nucl. Phys. A **217**, 589 (1973).
19. A.R. Junghans, M. de Jong, H.-G. Clerc *et al.*, Nucl. Phys. A **629**, 635 (1998).
20. V.M. Maslov, Yu.V. Porodzinskij, M. Baba, A. Hasegawa *et al.*, Eur. Phys. J. A **18**, 93 (2003).
21. W.P. Abfalterer *et al.*, Phys. Rev. C **63**, 044608 (2001).
22. A. Bohr, B. Mottelson, *Nuclear Structure*, Vol. **2** (Benjamin, New York, 1975).
23. A.V. Ignatjuk, K. Istekov, G.N. Smirenkin, Sov. J. Nucl. Phys. **29**, 450 (1979).
24. W.M. Howard, P. Möller, At. Data Nucl. Data Tables **25**, 219 (1980).
25. G. Hansen, A.S. Jensen, Nucl. Phys. A **406**, 236 (1983).
26. V.M. Maslov, Yu.V. Porodzinskij, JAERI-Research 98-038, Japan, 1998.
27. W.O. Myers, W.J. Swiatecki, Ark. Fys. **36**, 343 (1967).
28. S. Bjørnholm, J.E. Lynn, Rev. Mod. Phys. **52**, 725 (1980).
29. K.-H. Schmidt *et al.*, Nucl. Phys. A **665**, 221 (2000).
30. V.M. Maslov, in *Handbook for Calculations of Nuclear Reaction Data: Reference input parameter library*, IAEA-TECDOC-1034 (IAEA, Vienna, 1998) p. 81.
31. V.M. Maslov, INDC(BLR)-013, IAEA, Vienna, 1998.
32. W.P. Poenitz, Nucl. Sci. Eng. **64**, 89 (1977).
33. J.B. Czirr, J.B. Sidhu, Nucl. Sci. Eng. **57**, 18 (1975).
34. B. Leungers, S. Cierjacks, P. Brotz *et al.*, in *Proceedings of the NEANDC/NEACRP Specialists Meeting on Fast Neutron Fission Cross Sections ^{233}U , ^{235}U , ^{238}U and ^{239}Pu (USA, Argonne, 1976)*, ANL-79-90 (Argonne National Laboratory, 1976) p. 183.
35. G.W. Carlson, J.W. Behrens, Nucl. Sci. Eng. **66**, 205 (1978).
36. V.N. Dushin, A.V. Fomichev, S.S. Kovalenko *et al.*, At. Energ. **55**, (4), 218 (1983).
37. V.M. Adamov, B.M. Aleksandrov, I.D. Alkhozov *et al.*, Yad. Konstany **24**, 8 (1977).
38. K.R. Zasadny, H.M. Agrawal, M. Mahdavi, G.F. Knoll, Trans. Am. Nucl. Soc. **47**, 425 (1984).
39. V.A. Kalinin, S.S. Kovalenko, V.N. Kuz'min *et al.*, Vopr. At. Nauki Tekh. (Ser. Yad. Konstany) **4**, 3 (1987).
40. W. Younes, J.A. Becker, L.A. Bernstein *et al.*, Phys. Rev. C **64**, 044607 (2001).